Color Modulation in Morpho Butterfly Wings Using Liquid Crystalline Elastomers

ADVANCED INTELLIGENT SYSTEMS
Open Access
www.advintellsyst.com

Color Modulation in *Morpho* Butterfly Wings Using Liquid Crystalline Elastomers

Isabella De Bellis, Bin Ni, Daniele Martella, Camilla Parmeggiani, Patrick Keller, Diederik S. Wiersma, Min-Hui Li, and Sara Nocentini**

Nature provides well-engineered and evolutionary optimized examples of brilliant structural colors in animals and plants. *Morpho* butterflies are among the well-known species possessing iridescent bright blue coloration due to multiple optical effects generated by the complex structuration of the wing scales. Such surprising solution can be replicated to fabricate efficient devices. Maybe even more interesting, novel approaches can be developed to combine wings with synthetic smart materials to achieve complex structures responsive to external stimuli. This study demonstrates the proof of concept of an innovative biotic–abiotic hybrid smart structure made by the integration of a butterfly wing with thermoresponsive liquid crystalline elastomers, and their capability to actuate the mechanical action of the wing, thus controlling its spectral response. Exploiting two fabrication strategies, it is demonstrated how different mechanisms of color tuning can be achieved by temperature control. In addition, due to the thermally induced mechanical deformation of the elastomer and superhydrophobic properties of the wing, a potential self-cleaning behavior of the bilayer material is demonstrated.

1. Introduction

The study of evolutionarily optimized solutions of animals and plants is used in biologically inspired engineering to find inspiration for the development of better devices and technology. In nature, the morphology of living systems is responsible not only for the biological functions but frequently also for their appearance. A fascinating feature based on material architecture is that of structural coloration, which receives growing interest for the development of efficient reflective coatings, photonic devices, and optical sensors.[1–3]

An inspiring example is provided by the nanoarchitecture of the butterfly wings. Among them, the color of *Morpho menelaus*[4–6] is mainly determined by the interaction of light with the wing's complex scale morphology that produces a brilliant blue structural color as a sum of multiple optical effects. A specific characteristic of this species is the low angular dependence of wing coloration that remains bluish over a wide range of viewing angles, in contrast to what is typically observed in many other structural colors.[7] This unique property motivated a profound exploration of the morphology of the wing scales that are constituted by nanostructured cover and ground scales. The scales are nanostructured in ridges with a lamellar structure

I. De Bellis, Dr. D. Martella, Dr. C. Parmeggiani, Prof. D. S. Wiersma, Dr. S. Nocentini
European Laboratory for Non-Linear Spectroscopy (LENS)
University of Florence
via Nello Carrara 1, Sesto Fiorentino 50019, Italy
E-mail: nocentini@lens.unifi.it

B. Ni, Dr. M.-H. Li
Institut de Recherche de Chimie Paris
Chimie ParisTech, PSL University Paris, CNRS, UMR8247
11 rue Pierre et Marie Curie, Paris 75005, France
E-mail: min-hui.li@chimieparistech.psl.eu

Dr. D. Martella, Prof. D. S. Wiersma
Department of Physics and Astronomy
University of Florence
Via Sansone 1, Sesto Fiorentino 50019, Italy

The ORCID identification number(s) for the author(s) of this article can be found under https://doi.org/10.1002/aisy.202000035.

DOI: 10.1002/aisy.202000035

Dr. C. Parmeggiani
Department of Chemistry "Ugo Schiff"
University of Florence
via della Lastruccia 3-13, Sesto Fiorentino 50019, Italy

Dr. P. Keller
Laboratoire Physico-Chimie Curie
Institut Curie, UMR168
11 rue Pierre et Marie Curie, Paris 75005, France

Prof. D. S. Wiersma, Dr. S. Nocentini
Metrological Division of Novel Materials and Life Science
Istituto Nazionale di Ricerca Metrologica INRiM
Strada delle Cacce 91, Turin 10135, Italy

Dr. M.-H. Li
Beijing Advanced Innovation Center for Soft Matter Science and Engineering
Beijing University of Chemical Technology
15 North Third Ring Road, Chaoyang District, Beijing 100029, China

("Christmas tree"-like structure) with slightly different periodicity and a certain ridge height distribution.[4] Such complex quasiperiodic arrangement rules the *Morpho* butterfly appearance: a quasi-multilayer interference at the lamellae level combines with diffraction of the ridges creating a brilliant slightly angle-dependent iridescence.[5]

Morpho species have been classified according to the overlapping of ground and cover scales and the number of lamellae.[6] For *Morpho* species with a ridge morphology constituted by a small number (three or four) of lamellae, a successful replica has been reported using ferroelectric ceramic materials that, however, do not offer any tunability effects.[8] Although many strategies have been reported aiming at replicating the butterfly structure,[9–13] a faithful replica of the more complex morphologies (characterized by the multiscale periodicity of the *M. menelaus* butterfly scales, and the aspect ratio of its 3D nanostructuration) is still missing. Moreover, to obtain a tunable structural colored surface, soft deformable materials, as polydimethylsiloxane (PDMS) mold or liquid crystalline elastomers (LCEs), should be envisioned for the replica of the butterfly. Achieving this goal would open new routes for photonic applications, sensing applications, tunable colors, and colorful hydrophobic coating.[11,14,15]

Aiming at a responsive tunable optical platform, *Morpho* butterfly wings were demonstrated to be suitable not only as a template but also as a main constituent of integrated responsive devices. By coating the *Morpho* wing with photoresponsive linear polymers, a light-induced color change with a 70 nm blue shift has been demonstrated.[16] In sensing application, a biohybrid platform made by a multilayered structure of cardiomyocytes and carbon nanotubes superimposed to the butterfly wing showed a relevant color variation in response to the beating of cardiac muscle cells.[17] In both cases, polymers or cardiomyocytes and carbon nanotubes were placed on the top face of the wing with multiscale periodic structures. Consequently, the appearance of the butterfly wing is strongly affected by the coating layers that change the structural coloration by modifying the refractive index contrast.

To preserve the natural coloration of the *Morpho* butterfly, we present here an assembled hybrid system made by the butterfly wing and an artificial muscle based on LCEs, where LCEs were placed on the back side of the wing, thus keeping the color-generating top face free of contamination. This hybrid system benefits from both the optimized reflectance of the butterfly wing and the large and easily controllable contraction/expansion of the LCE artificial muscles. Such biotic–abiotic composite materials provide not only a mechanical actuation to tune the optical properties of the wings but also a deeper insight in the mechanism underlying the principle of the coloration of the *Morpho* butterfly. Moreover, such integration explores a new route for functional optical devices where an optimized photonic architecture can be coupled to a stimuli responsive material to tune the optical properties. In our study, a natural optimized platform was used, but this approach could be further extended to other devices with selective reflection properties such as Bragg multilayers,[2] flexible metal coatings, and photonic crystals.[18]

The remarkable property of LCE artificial muscles[19–25] is their shape change under an external stimulus such as temperature variation or light illumination. Taking advantage of their responsiveness to different stimuli and specifically to light,[25,26] they have been extensively explored in many research fields, from robotics,[27,28] to microfluidics,[29] and photonics.[30] Within the latter, LCE deformable elements can be used as actuators to remotely control the position of optical components as a mirror to steer a beam toward different adjacent directions,[31] or they can work themselves as photonic materials whose refractive indexes and shape can be dynamically tuned by light.[32,33] Furthermore, an example of hybrid material composed by LCEs and a synthetic photonic crystal (a silica opal) has been recently described,[34] whereas the interplay of LCE with natural structural color has been rarely explored.[16]

In this study, the used artificial muscles are nematic LCEs made of slightly cross-linked main-chain LC polymers. The principle of artificial muscle's contraction/elongation resides in the conformational change of the nematic LC polymer chain upon nematic (N)–isotropic (I) phase transition at T_{NI}. In the LC phase, the conformation of the macromolecular backbone is coupled with the orientational order of the mesogen units. In the nematic phase, the orientated mesogens force the polymer chains to stretch along the direction of the orientation.[35–37] However, when the transition from nematic to isotropic phase takes place, the orientational order is lost; consequently, the polymer chains can go back to the usual random coil conformation. Meanwhile, due to the cross-linked network, the orientational order of mesogens and the elongation of polymer chains can be restored to their original states at the nematic phase temperature. In an aligned macroscopic sample (monodomain), this reversible conformational change of polymer chains results in the reversible macroscopic shape change of LCEs, whose contraction/elongation behaves similar to real muscles.

The control over the structural color of the *Morpho* butterfly is achieved by exploiting two different LCE coupling strategies. LCE film can be first prepared by photopolymerization and then paired on the back and uncolored side of the *Morpho* wing. This way, the color variation induced by the natural wing flapping is reproduced upon thermally activated contraction/elongation of the LCE film (effect on the macroscale). Alternatively, thin LCE film can be prepared in situ by direct infiltration of monomeric mixtures in the wings' back side followed by polymerization in their aligned state. A local deformation of the scales' dimensions and nanostructuration is thus achieved (the effect on the nanoscale). In the former approach, the mechanical energy obtained by the thermosensitive deformation of the LCEs is used to reversibly control wing flapping, changing the resultant structural coloration for a fixed viewing angle. Interestingly, the variation of the contact angle is also observed, which has been exploited to control liquid droplet rolling along the ridge direction. In the latter approach, LCEs allow to elastically deform the single scale and the nanostructure periodicity that is thus responsible for the blue shift of the reflectance peak. In brief, the assembled biotic–abiotic hybrid system described here affords a smart multifunctional platform that shows structural color tuning and droplet motion on its superhydrophobic surface in response to temperature variation.

2. Results and Discussion

2.1. *M. Menelaus* Blue Butterfly: Morphology and Reflectance Characterization

In this work, a highly iridescent butterfly species, *M. menelaus*, was studied (**Figure 1**a) which has a bright blue coloration with a particular viewing angle dependence of the wing color. The nanostructured morphology determines an extremely high reflection, which strongly depends on the wavelength, the polarization state, the angle of incidence, and the refractive index of the ambient medium.[5] *M. menelaus* butterfly wing has two types of scales (cover and ground scales, as shown in Figure 1b,c), both of which have straight ridges of a height of 2–3 μm, separated by a distance of about 1 μm.[38] Both cover and ground scale ridges are characterized by a lamellar structure that determines the *Morpho* butterfly iridescence.

The nanometric structure has been characterized using scanning electron microscope (SEM) images shown in Figure 1d–f. The ground scales have a rectangular shape, whose typical size is 160 μm in length and 90 μm in width. Cover and ground scales are attached to the wing membrane alternately through holes called sockets. The shape of the cover scales varies from species to species. In *M. menelaus*, the shape is quasirectangular, but the lateral size is shorter. If the singular scales are observed in transmission (Figure S1, Supporting Information), the cover scale looks transparent, whereas the ground scale looks dark brown, meaning that the presence of a pigment also contributes to the overall coloration. Each scale is characterized by ridges (or vanes) aligned along the long size of the scale whose periodicity mainly affects the butterfly appearance. The distance between adjacent ridges of the cover scale is ≈1700 nm (Figure 1d), whereas in the ground scales the vanes are ≈700 nm apart (Figure 1e). The two scales have a different role in the color determination: the cover scale mostly diffuses light, whereas the ground scale is responsible for the structural color. The superposition of the two determines the blue coloration.[39] Considering a white light illumination at 45° with with respect to wing normal (Figure S2a, Supporting Information), an in-plane rotation (in the wing plane) shows that the reflectance depends on the orientation of the scale with respect to the illumination direction (Figure S2b, Supporting Information).

A careful observation of the ground-scale morphology shows that each ridge has a laminated structure of several lamellae superimposed on each other and slightly tilted on the scale plane (Figure 1f and Figure S3a, Supporting Information). From an optical point of view, these scales behave like a 2D periodic structure. In the scale plane, previous characterizations report that a ridge separation of 600 nm (in our sample, 700 nm) results in a diffraction effect, whereas the lamellae of a mean thickness of 100 nm (in our case, 110 nm) produce interference effects in the blue part of the visible spectrum.[40]

To calculate the peak wavelength of the reflectance, we used a simple 1D optical calculation based on the configuration of multilayer thin-film interference (Figure S3b, Supporting Information), obtaining the reflectance peak at 478 ± 18 nm. Such estimation has been compared with the experimentally measured reflectance whose maximum value is about 55% at 483 ± 1 nm. The peak wavelength corresponds to a vivid blue coloration. This maximal reflectance wavelength is not constant all over the entire wing, as every point has a slightly diverse geometry and therefore a spectral response whose maximum value is in the range of 460–500 nm. In Figure S4a of the Supporting Information, we report the reflectance for another wing point whose peak is at 487 ± 1 nm. In our characterizations, we fixed the wing point under analysis and thus observed the induced color shift induced by the different effects. It is interesting to note in Figure S4b of the Supporting Information, that the reflectance wavelength maximum is highly sensitive to minute lamellae thickness variations: fixing the air spacing at 65 nm, a 10 nm lamella thickness increase leads to a pronounced spectrum red shift up to 503 nm showing as few

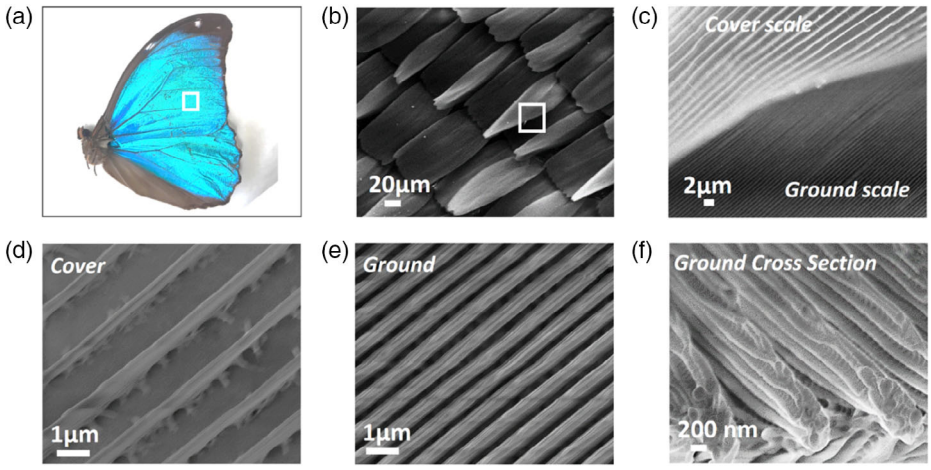

Figure 1. a) *M. menelaus* blue butterfly. b) SEM image. The ground scales have a rectangular shape and a typical size of 160 μm in length and 90 μm in width, whereas the cover scales have a quasirectangular shape and a reduced lateral size. c) SEM image magnification of ground and cover scale detail. Both scales show a periodic arrangement of longitudinal vanes (or ridges). d) SEM image of cover scale vanes showing 1700 nm separation between adjacent ridges. e) SEM image of ground scale vanes showing 700 nm separation between adjacent ridges. f) A lateral SEM image of the ridges of the ground scale cross-section, showing structures with overlapping lamellae.

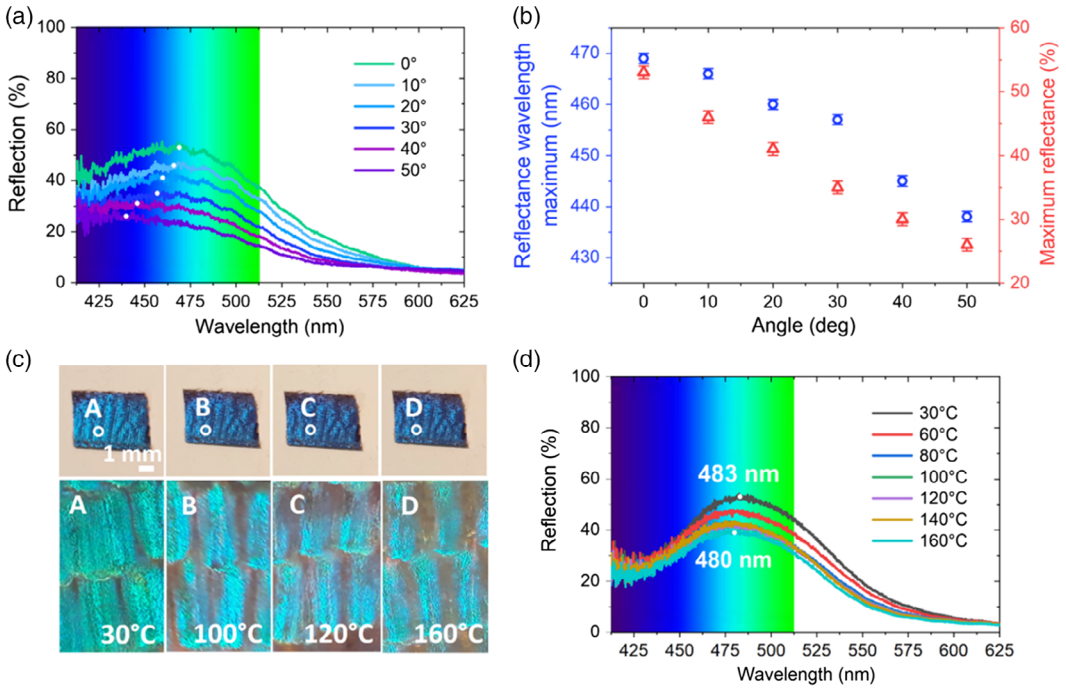

Figure 2. a) Reflectance spectra of the original flat wing tilted from 0° to 50° with step of 10°. b) Tilting angle dependence of the reflectance spectrum peak and its maximum intensity. c) *Morpho* butterfly appearance monitored by an optical microscope (equipped with a 10× objective) in a temperature range from 30 to 160 °C. No significant color variation can be observed. d) Reflectance spectra of a single point of the original wing changing the temperature from 30 to 160 °C.

nanometers can create a pronounced blue or a red shift of the reflectance maximum.

The spectral characterization was done using the optical setup shown in Figure S5a of the Supporting Information. To characterize the wing iridescence, the sample has been tilted at different angles from 0° to 50° with steps of 10° (**Figure 2**a and Figure S5b, Supporting Information), keeping fixed the illumination and collection direction. The sample was always oriented with the scale ridges perpendicular to the plane of incident light because reflectance is higher in this configuration.[41] The wavelength shift and the maximum intensity of the reflectance as a function of the tilting angle show as increasing the angle, a progressive blue shift occurs from 469 ± 1 nm at 0° to 438 ± 1 nm at 50° together with the reflectance reduction from 53% to 26% (Figure 2b). Similar values have been previously measured and reported in the literature.[42]

As we aimed to make a thermoresponsive biotic–abiotic assembly, we first measured the reflectance of the butterfly wing as a function of temperature. The appearance of *Morpho* butterfly was monitored by an optical microscope (equipped with a 10× objective) in a temperature range from 30 to 160 °C (Figure 2c).

We can suppose that the thermal expansion causes an increase in spacing between the ridges, an expansion of the lamellar structure and a thermally induced reduction in the refractive index of chitin.[43] It has been noted that the contribution of the refractive index variation and expansion of the tree-like lamellar structure can be neglected,[44] whereas the dominant effect should be attributed to the increasing spacing between the ridges. No significant color variation can be observed as was confirmed by the reflectance spectra measured and shown in Figure 2d that do not show a spectral shift (the lamellae separation remains unvaried) but only a reflectance efficiency decrease due to a constructive interference reduction.

2.2. Biotic–Abiotic Hybrid System Made by *M. Menelaus* Blue Butterfly and LCE Artificial Muscle

To obtain a thermosensitive mechanical control on the wing properties, we used LCE artificial muscles made by photopolymerization of a thiol-ene/acrylate formulation.[42] The molecular structures of all components are shown in Figure S6 of the Supporting Information, which are similar to a formulation described previously,[45] but slightly different in spacer lengths of LC monomers. Note that to get enough mechanical actuation, LCE muscles of 160 μm and 1 mm thickness were prepared and the detailed process is described elsewhere.[46] In our applications, the LCE films has been prepared from LC monomeric mixtures homogenously aligned by the magnetic field between two permanent magnets. After such alignment procedure, the polymerization has been performed by UV irradiation at room temperature at which the LC monomeric mixture is in the nematic phase. Typically, the obtained LCE exhibits a contraction of 50% along the direction of alignment when heating from 30 to 150 °C with a steep contraction around nematic to isotropic phase transition ($T_{NI} = 120$ °C), as shown in Figure S7 of the Supporting Information, and **Figure 3**a.

The piece of LCE muscle as shown in Figure 3a is then glued on the back of a piece of wing cut in a cross shape (Figure 3b) or a rectangular shape (Figure 3c).

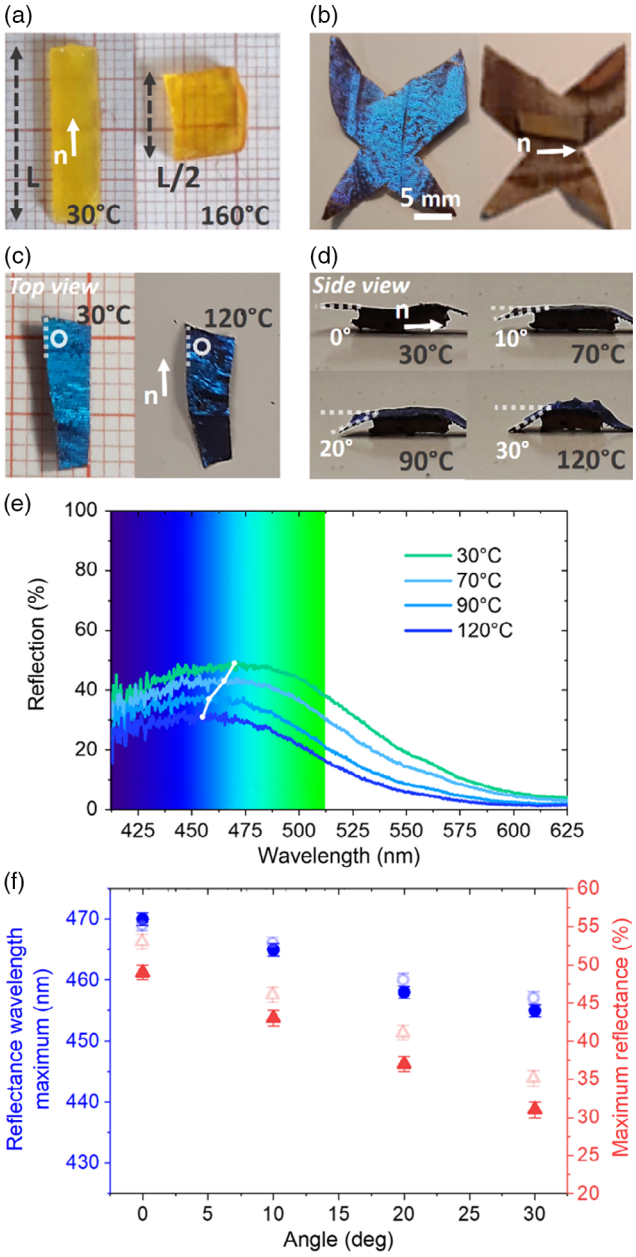

Figure 3. a) LCE film with a thickness of 1 mm at 30 and 160 °C. The slight opacity of the LCE film is because of the rather high thickness of the film (1 mm) and the nonperfect monodomain alignment, which however do not affect the big deformation of the sample. A small piece of the film was cut to be integrated underneath the ventral (back) side of the butterfly. b) LCE film integration on the back side of a cross shape wing. LCE film integration on the back side of a rectangular shape wing with c) top view of hybrid system's contraction and color change and d) side view of hybrid system's bending upon heating from 30 to 120 °C. e) Reflectance spectra of the hybrid rectangular shape wing as a function of temperature. The reflection is collected from the end part of the wing stripe that shows a bending of 0°, 10°, 20°, and 30° at 30, 70, 90, and 120 °C, respectively. f) Reflectance wavelength maximum and maximum reflectance intensity of the hybrid rectangular shape wing as a function of the bending angle. Empty markers refer to the corresponding values for the original butterfly tilted at different angles.

Once integrated on the back of the wing, the contraction of a small piece of the LCE induces a thermomechanical stress on the butterfly wing (whose surface area is larger than the actuator one; Figure 3c). In response to different temperatures, a gradual shape change of the film is obtained leading to the angular control of the butterfly wing flapping (Figure 3d). While at room temperature, the wing lays flat over the elastomeric actuator, increasing the temperature, it bends up to 30° once the film is heated at 120 °C. If the reflectance of the bent part of the wing is monitored, a blue shift of 15 nm is observed, and the value of the reflectance reduces by 18% (Figure 3e,f). Comparing such values with the ones obtained by the angular measurement for the *Morpho* butterfly wing without the LCE actuator (Figure 2b), as shown in Figure 3f, allows us to explain the spectral shift as a change in coloration induced by the butterfly iridescence at different bending angles. The small difference between the two measured spectral shifts can be attributed to an inaccuracy in the angle measurement and a not perfect flat bending of the wing.

The hierarchical micro-/nanostructuration of the scales also generates a superhydrophobic platform. The thermal control of the angular bending of the butterfly piece induces not only a blue shift of the color surface but also a self-cleaning effect (**Figure 4**a), which is independent on the cut wing shape. The drop contact angle variation in forward and backward direction is shown in Figure 4a,b as a function of the increasing temperature up to 160 °C. At room temperature, a small difference between the advancing and receding angles (low contact angle hysteresis defined as the rose petal effect) does not perturb the droplet position, while increasing such difference up to 80 °C the drop starts to roll out along the ridges until it slides out of the butterfly. Figure S8 of the Supporting Information, shows as in response to different temperatures, a gradual shape change of the rectangular wing induces the sliding of a glycerol drop on its surface. In Figure 4c, two different glycerol drops (A and B), placed on the cross shape wing, exhibit anisotropy in the sliding direction.[47] Indeed, a droplet easily rolls along the radial outward (RO) direction (denoted by the arrow in the SEM image of Figure 4d) but is tightly pinned in the orthogonal direction (perpendicular to the scale vanes). The macroscopic LCE contraction induces the droplet A sliding along the parallel groove microstructures, whereas droplet B remains pinned as the wing curling would mostly favor its motion along the direction perpendicular to RO. A SEM magnification of a cover scale detail is shown in Figure 4d highlighting the RO direction.

To improve the coupling between the two components and the protocol reproducibility, direct infiltration of the mixture of LC molecules on the back side of the wings was evaluated. Here, the LC monomeric mixture is placed on the uncolored back side of a wing stripe and diffuses along the ridges by capillary forces creating a thin layer of less than a few microns. In such a way, we obtained a quite homogenous film that covers the brown and jagged scales of the ventral side of the wing without affecting the natural photonic structure (present on the upper surface). The ventral wing membrane where scales are inserted into sockets (Figure S9a, Supporting Information) further prevents the LC monomeric mixture infiltration among the scales of the dorsal upper side. The LC monomeric mixture has been first homogeneously aligned along the direction perpendicular to the scale length and vanes direction by two magnets, and then

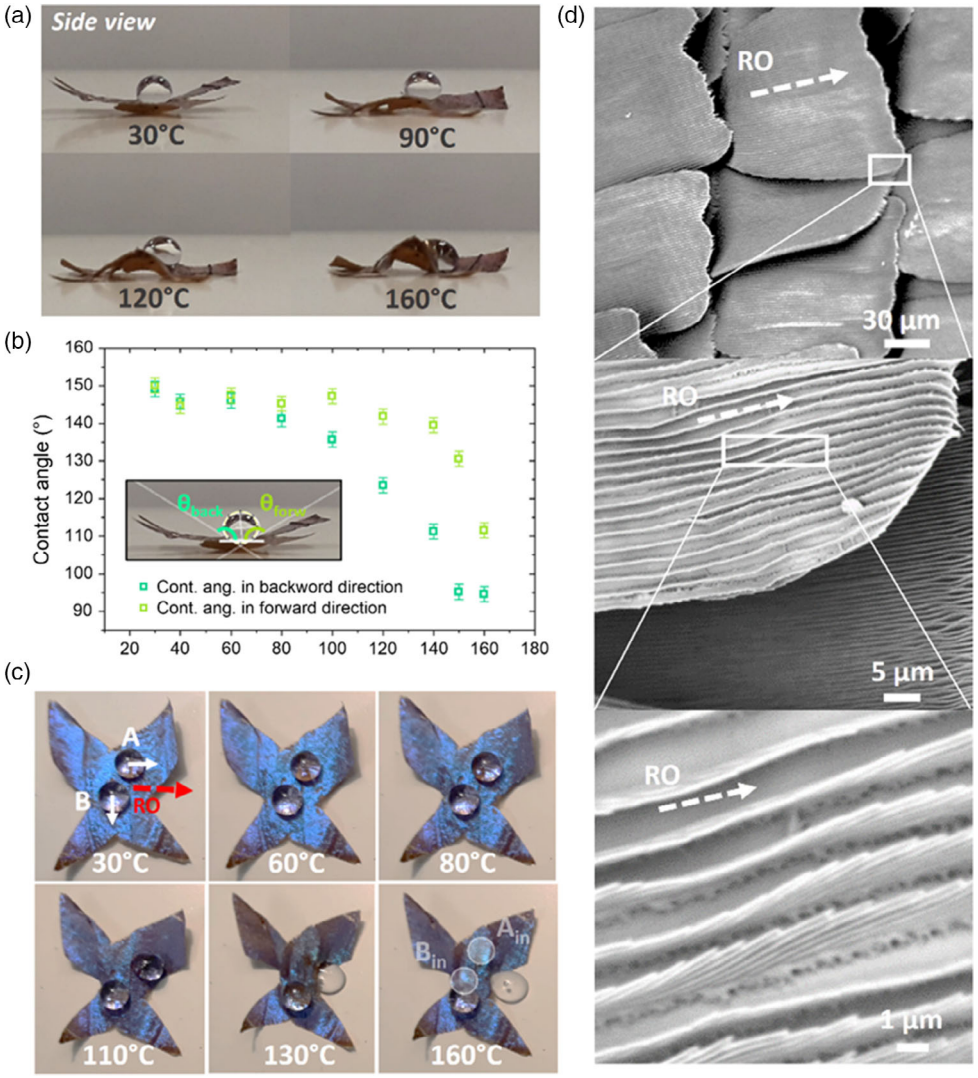

Figure 4. a) Side view of a glycerol drop sliding along the longitudinal vanes direction when the hybrid cross-shape wing is activated and deformed by heat. b) Contact-angle variation in backward and forward direction (advancing and receding contact-angle measurement) of the glycerol drop as a function of temperature. c) Movement of drops A and B during the butterfly deformation at different temperatures. Drop A slides out of the wing because it is rolling along the vanes direction. The initial positions of the droplets (A_{in} and B_{in}) are marked for reference in the image taken at 160 °C. d) SEM images of cover scales for different magnifications. The arrow in the SEM images denotes the RO direction along which a drop slides easily.

polymerized and cross-linked under UV irradiation.[48,49] **Figure 5**a shows the optical image of the back of the hybrid sample (piece of wing with infiltrated LCE) in which the director **n** indicates the direction of the molecular alignment. The good alignment homogeneity of the final LCE layer is shown in the SEM images (Figure 5b) with different magnifications, whereas the LCE alignment has been verified by a polarized optical microscope (POM) images as shown in Figure 5c where the transmittance extinction is observed for sample rotation of 45°, while in case of the untreated original butterfly no color intensity variation was observed.

Looking at the microscope images of each single ground scale in Figure 5d, the untreated wing, reported on the left panels, has no scale deformation increasing temperature up to 160 °C. In the same temperature range instead, the hybrid LCE infiltrated system at 30 °C (on the top right) shows a 10% width scale contraction due to an initial strain induced by the polymerization of the LC monomeric mixture, and the increase in temperature up to 160 °C leads to a further size reduction of 15% (on the bottom right). The underlying LCE layer induces a slightly curved shape at the stripe edges at room temperature, which is lost at 80 °C when the system flattens out (Figure 5e and Figure S9b, Supporting Information). This effect is absent in the untreated butterfly that shows a negligible bending behavior when it is heated as no external stress is present. The bilayered system thus returns in a reversible way to its initial shape in 70 s when room temperature is restored (Figure S9c, Supporting Information). The slight deformation variations of the different points of the wing can be attributed to some inhomogeneities of the LCE film thickness (Figure S10, Supporting Information).

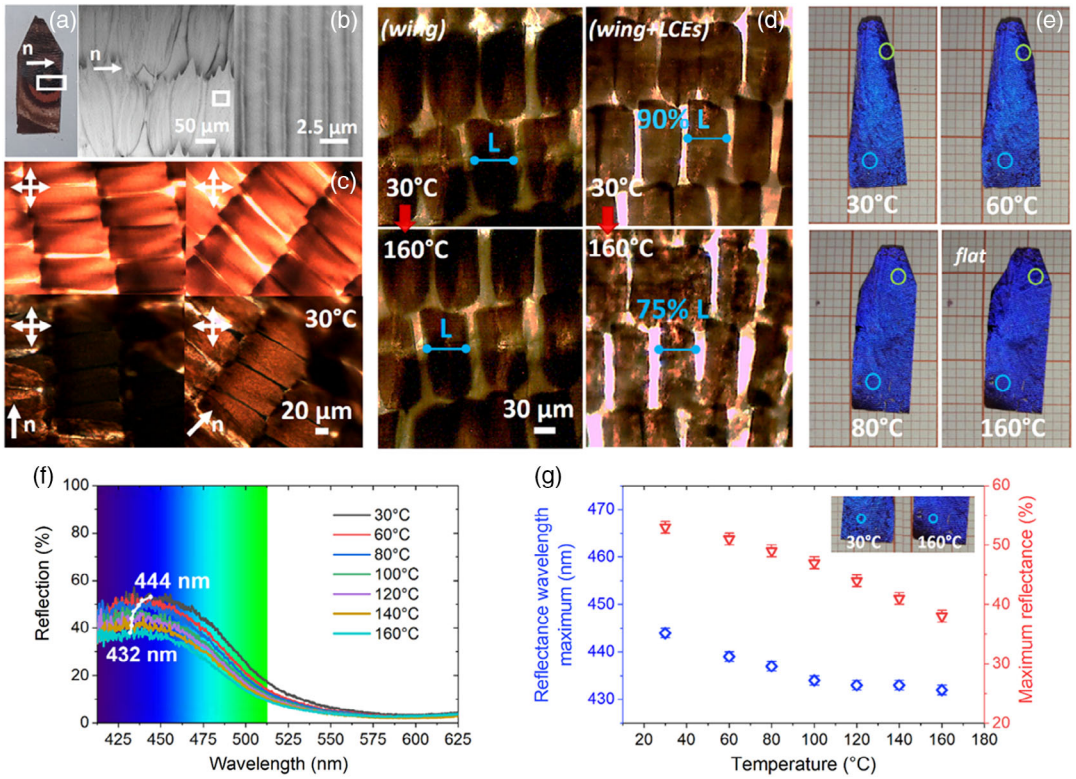

Figure 5. a) Optical image of the back side of the wing with infiltrated LCE after UV polymerization. The nematic director is indicated by the vector, **n**. b) SEM images of the LCE layer. c) POM images of the untreated butterfly wing (two images on the top) and of the wing with infiltrated LCE on its back side (two images on the bottom). Cross arrows represent the directions of polarizer and analyzer. d) Optical images of the untreated butterfly (two images on the left) and the wing with infiltrated LCEs (two images on the right) at 30 °C and at 160 °C. In the first case, no deformation of the ground scales has been observed. In the second case, a 10% deformation has been observed after the polymerization of LC monomeric mixture and a further 15% contraction has been measured when heated at 160 °C. e) The hybrid system has a convex curled shape at room temperature and reaches a flat shape, with the increase in temperature, due to the LCE layer strain and deformation. f) Reflectance spectra of the hybrid structure at different temperatures. The reflection is collected from the flat part of the wing stripe. g) Reflectance wavelength maximum and maximum reflectance intensity as a function of temperature collected from flat part of the butterfly wing (the inset at 30 and 160 °C).

To investigate the LCE role, we measured the reflectance spectra of the flat part of the sample (Figure 5f), indicated with a light blue circle in Figure 5e, for different values of temperature in between 30 and 160 °C, also reporting the maximum peak of every reflective spectrum and the intensity as a function of temperature in Figure 5g.

During the thermal actuation, the monitored part remains flat which means that the contribution to the reflectance shift cannot be attributed to the iridescence of the sample. At room temperature, the LCE stress reflects in a blue shift of 39 nm with respect to the untreated butterfly wing reflectance. By increasing the temperature above 100 °C, the lateral contraction of each single scale modifies the nanostructured ridges inducing a wavelength shift of 12 nm. A total shift of 51 nm with respect to the untreated butterfly has been thus obtained. This color tuning can be attributed not only to the ridge distance variation but also to a tilting and/or bending of the ridges due to the LCEs strain. Such phenomena resulted in the decrease in the air separation between the lamellae and thus in a different interference effect of the stack. To explore the different contribution of the geometrical parameter of the periodic ridges, we performed reflectance calculation of the periodic tree structure using a MATLAB code for periodic patterned multilayers based on rigorous coupled wave analysis (RCWA).[50–52] The periodic unit cell represents the tree structured ridge with the geometrical dimensions measured in the SEM images of Figure S3 of the Supporting Information.

The reflection spectrum has been calculated and shown in **Figure 6**a considering the case of a ten lamellae stack using a simplified model based on multilayer interference effect, in which the lamellae are considered perfectly parallel to the membrane substrate and symmetrically distributed with respect to the ridge trunk (the inset in Figure 6a). The calculation results show a reflection peak at around 480 nm (blue color), greatly reproducing the experimentally measured reflectance, and other two weak peaks at about 420 and 560 nm. Monitoring the squared electric field distribution within each ridge at 400, 480, and 600 nm (Figure 6b), we could better understand the photonic properties of the butterfly. At 400 nm, the lamellar structure determines a not-optimized reflection and a relatively weak transmission through the tree-like structure with a weak cavity effect within each ridge. At the reflectance maximum, the periodic structure behaves as an effective Bragg reflector explaining the strong

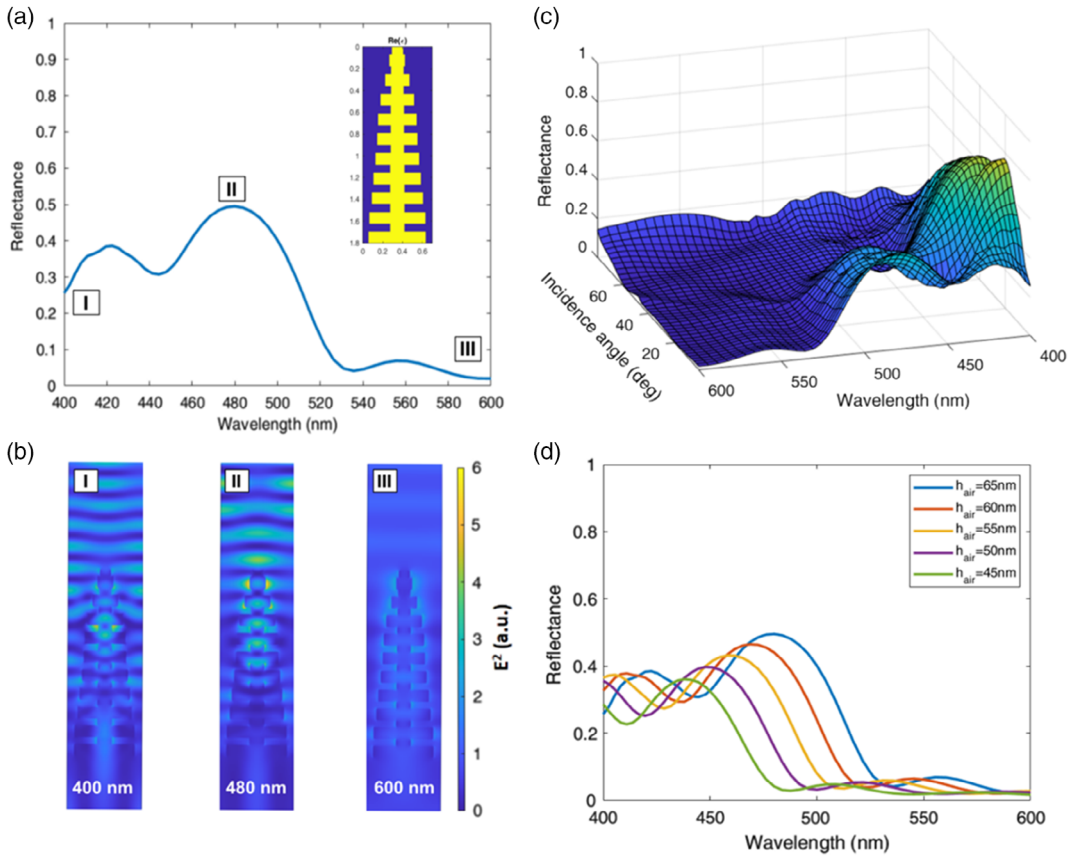

Figure 6. a) Calculation of the reflectance spectrum from the tree-like structure of the scale ridges with ten lamellae layers. In the inset, the periodic unit cell of the RCWA calculation is reported. b) Squared electric field spatial distribution for three different wavelengths: 400, 480, and 600 nm. c) Reflectance dependence on the angular direction of the incident wave. The incident angle is calculated with respect to the normal to the scale surface. d) Calculations of reflectance spectrum varying the thickness of the air layer between the lamellae.

reflection peak in the blue spectral range. Increasing the wavelength up to 600 nm, the nanometric periodicity does not affect anymore the light propagation that is mostly transmitted across the scale leading to a negligible reflectance.

As expected for Bragg reflectors, increasing the angle of incidence of the plane wave with respect to the normal to the surface, a blue shift of the reflectance occurs as reported in the reflectance map as a function of the light incidence angle in Figure 6c. Focusing on the contribution of the scale parameter variation while actuating the infiltrated LCE layer, we calculated the reflectance spectra singularly varying the pitch of the ridges, the thickness of the lamellae, and their interspacing. Interestingly, a reduction of the ridge separation (Figure S11a, Supporting Information) induces a blue shift of the spectra and a more pronounced reflection intensity, probably due to an effective refractive index increase and interference effect. Contrary to previously reported assumption,[14] we exclude that both the experimental initial shift of 39 nm and the minor shift of 12 nm could be attributed to the lamellae contraction, as in this case an effective blue shift will be expected without an intensity reflectance variation, as demonstrated in the calculation of Figure S11b of the Supporting Information. We rather suppose that the LCE strain and activation generate both a gradual approach of the vanes together with a slight deformation of each single ridge. As shown in Figure 6d, reporting the reflectance spectra calculated when the air layer thickness changed from 65 to 45 nm, a blue shift of about 50 nm with an intensity decrease from 50% to 38% is observed. This result is in complete agreement with the experimental measurements as shown in Figure 5f, and indicates that the color tuning is mostly determined by the variation of the air space between chitin lamellae.

Monitoring instead the color tuning at the bent edges of the assembled wing stripe (Figure S12, Supporting Information), a combined contribution of the ridge separation variation and iridescence can be progressively appreciated increasing the temperature.

3. Conclusions

Nature provides complex systems with extraordinary features that can be sometimes combined with synthetic materials for a more efficient control and toward the exploration of more complex behavior. This would ask for a deep understanding of the materials (both natural and synthetic ones), together with the full achievement of the best practices to combine them. Due to the

achievement of the aforementioned points, a hybrid system composed by the butterfly wing and a LCE artificial muscle has been demonstrated as a smart temperature-responsive platform with different functionalities.

Structural color tuning in *Morpho* butterfly wing was obtained by the integration of a thermoresponsive LCE actuator following two different coupling strategies: one using a LCE millimetric film actuator stuck to the back side of the wing, and the other one by means of an underlying infiltrated LCE layer. The first strategy leads to a 15 nm blue shift that is thermomechanically induced by the iridescence change of the flapping wing. Such color tuning can also be combined with the superhydrophobic properties of the nanostructured wing scales on which a glycerol droplet rolls out by temperature variation, creating a natural/synthetic platform for self-cleaning applications.

Following the second strategy, an initial blue shift of the reflectance with respect to the untreated butterfly, induced by a stress of the polymerized layer in the back side of the wing, has been first measured at room temperature. During thermal actuation of the LCE muscle up to 80 °C, the wing stripe returns to flat shape (by thermal relaxation of the stress) and then remains flat upon further heating to 160 °C. Together with this thermally driven deformation, the scales dimension shrinks down to 75% of their natural value in their lateral size. Consequently, this effect leads to a blue shift that is not any more ruled by iridescence but only due to a nanostructure modification of the wing ridges. By a comparison of the measured spectra with the RCWA calculation results, we can conclude that the blue shift of the reflection peak can be attributed to the variation of the interspacing in between the lamellae of the scale ridges induced by the temperature-driven LCE strain. The thermosensitive properties of this biotic–abiotic platform would open to the first prototype of bio-synthetic responsive devices as visualizable thermal sensors. At the same time, the integration and actuation mechanism can be extended to other thin flexible reflectors and can drive further new structural color designs for responsive tunable platforms. Furthermore, by synthetic material optimization, responsiveness of the composite platforms can be shifted quite easily to different temperature ranges and/or different stimuli, such as light, that can be used to induce actuation toward smart self-tuning devices.

4. Experimental Section

LCE Film Preparation: LCE film was prepared using LC monomeric mixture as shown in Figure S6, Supporting Information.[46] Briefly, the mixture with photoinitiator Irgacure 369 was filled in a rectangular mold made of PDMS. Homogeneous alignment was obtained by the magnetic field between two permanent magnets upon cooling the LC monomeric mixture from isotropic phase (110 °C) to room temperature. The polymerization/cross-linking was achieved under UV light at room temperature.

LCE Film Integration in M. Menelaus Wing: A piece of the butterfly wing was cut with a blade, and a small amount of LC monomeric mixture (used as glue for the bilayer assembly) heated at 100 °C was gently placed on the back side of the wing. LCE film was placed on the LC monomeric mixture, which was then photopolymerized at room temperature for 60 min. This process was to ensure the adhesion of the LCE film to the back of butterfly wing. The use of a LCE film of a thickness of 1 mm allowed for a more efficient and symmetric control of the structure deformation with respect to the thinnest film of 160 µm as shown in Figure S13, Supporting Information.

LCE Layer Infiltrated in M. Menelaus Blue Butterfly Wing: The mixture of LC molecules was infiltrated at 100 °C on the brown ventral side of a wing stripe. The solid membrane, on which cover and ground scales were attached, prevented the LCE penetration inside the photonic structures, avoiding the natural refractive index contrast variation between air and chitin. The sample was then placed between two magnets and cooled until room temperature with a slow temperature ramp ($-1\ ^\circ C\ min^{-1}$) to align the LC molecules. The whole setup was placed in an oxygen-free environment flushed with a slow stream of argon to proceed the polymerization/cross-linking under UV light ($30\ mW\ cm^{-2}$ for 60 min).[45,46] Analysis by SEM showed homogenous elastomeric layer (Figure 5b and Figure S10a, Supporting Information).

Experimental Setup for Spectroscopic Measurement: The light emitted from a halogen lamp was first collimated through a system of lenses and then focused on the butterfly sample by a doublet lens (30 mm focal length). A 10× objective collected the reflected light that was analyzed by an Ocean Optics USB4000 spectrometer. We focused on the reflectance spectrum in the visible spectra range from 400 to 650 nm.

Supporting Information

Supporting Information is available from the Wiley Online Library or from the author.

Acknowledgements

We thank M. Hui Chen and Dr. Fan Sun (Chimie ParisTech) for their help in SEM imaging and Dr. Lorenzo Pattelli for his help on RCWA. Financial support from French National Research Agency (grant no. ANR-16-CE29-0028) and Ente Cassa di Risparmio di Firenze (grant nos. 2015/0781 and 2017/0881) are acknowledged. B.N. gratefully acknowledges the China Scholarship Council for funding his PhD scholarship. We thank Rémy Fert and Eric Nicolau (the machine shop at UMR 168 CNRS Curie) who built the two magnets setup used in the alignments.

Conflict of Interest

The authors declare no conflict of interest.

Keywords

biohybrid platforms, color tuning, liquid crystalline elastomers, *Morpho* butterfly, self-cleaning, superhydrophobicity, thermosensitive optical sensors

Received: February 28, 2020
Revised: May 9, 2020
Published online: June 14, 2020

[1] Q. Li, Q. Zeng, L. Shi, X. Zhang, K.-Q. Zhang, *J. Mater. Chem. C* **2016**, *4*, 1752.
[2] K. Chung, S. Yu, C.-J. Heo, J. W. Shim, S.-M. Yang, M. G. Han, H.-S. Lee, Y. Jin, S. Y. Lee, N. Park, J. H. Shin, *Adv. Mater.* **2012**, *24*, 2375.
[3] Q. Shen, J. He, M. Ni, C. Song, L. Zhou, H. Hu, R. Zhang, Z. Luo, G. Wang, P. Tao, *Small* **2015**, *11*, 5705.
[4] S. Kinoshita, S. Yoshioka, K. Kawagoe, *Proc. R. Soc. Ser. B* **2002**, *269*, 1417.
[5] S. Kinoshita, S. Yoshioka, J. Miyazaki, *Rep. Prog. Phys.* **2008**, *71*, 076401.

[6] M. A. Giraldo, S. Yoshioka, C. Liu, D. G. Stavenga, *J. Exp. Biol.* **2016**, *219*, 3936.
[7] S. Kinoshita, S. Yoshioka, *ChemPhysChem* **2005**, *6*, 1442.
[8] P. J. Vernon, Y. Fang, Y. Cai, K. H. Sandhage, *Angew. Chem. Int. Ed.* **2010**, *49*, 7765.
[9] S.-H. Kang, T.-Y. Tai, T.-H. Fang, *Curr. Appl. Phys.* **2010**, *10*, 625.
[10] H. Butt, A. K. Yetisen, D. Mistry, S. A. Khan, M. U. Hassan, S. H. Yun, *Adv. Opt. Mater.* **2016**, *4*, 497.
[11] R. E. Rodríguez, S. P. Agarwal, S. An, E. Kazyak, D. Das, W. Shang, R. Skye, T. Deng, N. P. Dasgupta, *ACS Appl. Mater. Interfaces* **2018**, *10*, 4614.
[12] S.-H. Kang, T.-Y. Tai, T.-H. Fa, *Curr. Appl. Phys.* **2010**, *10*, 625.
[13] S. Zhang, Y. Chen, *Sci. Rep.* **2015**, *5*, 16637.
[14] R. A. Potyrailo, R. K. Bonam, J. G. Hartley, T. A. Starkey, P. Vukusic, M. Vasudev, T. Bunning, R. R. Naik, Z. Tang, M. A. Palacios, M. Larsen, L. A. Le Tarte, J. C. Grande, S. Zhong, T. Deng, *Nat. Commun.* **2015**, *6*, 7959.
[15] R. H. Siddique, A. Faisala, R. Hnigb, C. Bartelsc, I. Wackerc, U. Lemmerb, H. Hölscher, *Proc. SPIE* **2014**, *9187*, 91870E.
[16] X. Qing, Y. Liu, J. Wei, R. Zheng, C. Zhu, Y. Yu, *Adv. Opt. Mater.* **2019**, *7*, 1801494.
[17] Z. Chen, F. Fu, Y. Yu, H. Wang, Y. Shang, Y. Zhao, *Adv. Mater.* **2018**, 1805431.
[18] M. E. Calvo, L. González-García, J. Parra-Barranco, A. Barranco, A. Jiméne-Solano, A. R. Gonzále-Elipe, H. Míguez, *Adv. Opt. Mater.* **2015**, *3*, 171.
[19] P.-G. de Gennes, *C. R. Acad. Sci.* **1975**, *281b*, 101.
[20] P.-G. de Gennes, *C. R. Acad. Sci.* **1997**, *324*, 343.
[21] J. Küpfer, H. Finkelmann, *Makromol. Chem. Rapid Commun.* **1991**, *12*, 717.
[22] H. Wermter, H. Finkelmann, *e-Polymers* **2001**, *013*, 1.
[23] M.-H. Li, P. Keller, *Phil. Trans. A* **2006**, *364*, 2763.
[24] T. Ikeda, J.-I. Mamiya, Y. Yu, *Angew. Chem. Int. Ed.* **2007**, *46*, 506.
[25] T. J. White, D. J. Broer, *Nat. Mater.* **2015**, *14*, 1087.
[26] Y. Yu, T. Ikeda, *Angew. Chem. Int. Ed.* **2006**, *45*, 5415.
[27] D. Martella, S. Nocentini, C. Parmeggiani, D. S. Wiersma, *Adv. Mater. Technol.* **2019**, *4*, 1800571.
[28] H. Zeng, P. Wasylczyk, D. S. Wiersma, A. Priimagi, *Adv. Mater.* **2018**, *30*, 1703554.
[29] A. H. Gelebart, M. Mc Bride, A. P. H. J. Schenning, C. N. Bowman, D. J. Broer, *Adv. Funct. Mater.* **2016**, *26*, 5322.
[30] S. Nocentini, D. Martella, C. Parmeggiani, D. S. Wiersma, *Adv. Opt. Mater.* **2019**, *7*, 1900156.
[31] S. Nocentini, D. Martella, D. S. Wiersma, C. Parmeggiani, *Soft Matter* **2017**, *13*, 8590.
[32] I. De Bellis, D. Martella, C. Parmeggiani, E. Pugliese, M. Locatelli, R. Meucci, D. S. Wiersma, S. Nocentini, *J. Phys. Chem. C* **2019**, *123*, 26522.
[33] S. Nocentini, D. Martella, C. Parmeggiani, S. Zanotto, D. S. Wiersma, *Adv. Opt. Mater.* **2018**, *6*, 1800167.
[34] H. Xing, J. Li, Y. Shi, J. Guo, J. Wei, *ACS Appl. Mater. Interfaces* **2016**, *8*, 9440.
[35] M. H. Li, A. Brûlet, P. Davidson, P. Keller, J. P. Cotton, *Phys. Rev. Lett.* **1993**, *70*, 2297.
[36] J. P. Cotton, F. Hardouin, *Prog. Polym. Sci.* **1997**, *22*, 795.
[37] D. J. Broer, J. Boven, G. N. Mol, G. Challa, *Makromol. Chem.* **1989**, *190*, 2255.
[38] S. Yoshioka, S. Kinoshita, *Proc. R. Soc. Ser. B* **2004**, *271*, 581.
[39] R. H. Siddique, S. Vignolini, C. Bartels, I. Wacker, H. Hölscher, *Sci. Rep.* **2016**, *6*, 36204.
[40] S. Berthier, E. Charron, A. Da Silva, *Opt. Comm.* **2003**, *228*, 349.
[41] S. Zobl, B. D. Wilts, W. Salvenmoser, P. Pölt, I. C. Gebeshuber, T. Schwerte, *Biomimetics* **2020**, *5*, 5.
[42] F. Liu, Y. Liu, L. Huang, X. Hu, B. Dong, W. Shi, Y. Xie, X. Ye, *Opt. Commun.* **2011**, *284*, 2376.
[43] S. Niu, B. Li, Z. Mu, M. Yang, J. Zhang, Z. Han, L. Ren, *J. Bionic Eng.* **2015**, *12*, 170.
[44] A. D. Pris, Y. Utturkar, C. Surman, W. G. Morris, A. Vert, S. Zalyubovskiy, T. Deng, H. T. Ghiradella, R. A. Potyrailo, *Nat. Photonics* **2012**, *6*, 195.
[45] T. H. Ware, Z. P. Perry, C. M. Middleton, S. T. Iacon, T. J. White, *ACS Macro Lett.* **2015**, *4*, 942.
[46] B. Ni, M. Zhang, C. Guyon, P. Keller, M. Tatoulian, M.-H. Li, unpublished.
[47] Y. Zheng, X. Gao, L. Jiang, *Soft Matter* **2007**, *3*, 178.
[48] M.-H. Li, P. Keller, J.-Y. Yang, P.-A. Albouy, *Adv. Mater.* **2004**, *16*, 1922.
[49] A. Buguin, M.-H. Li, P. Silberzan, B. Ladoux, P. Keller, *J. Am. Chem. Soc.* **2006**, *128*, 1088.
[50] Simone Zanotto 2020. PPML – Periodically Patterned Multi Layer, https://www.mathworks.com/matlabcentral/fileexchange/55401-ppml-periodically-patterned-multi-layer, MATLAB Central File Exchange (accessed: December 2019).
[51] S. Zanotto, G. Mazzamuto, F. Riboli, G. Biasiol, G. C. La Rocca, A. Tredicucci, A. Pitanti, *Nanophotonics* **2019**.
[52] S. Zanotto, F. Sgrignuoli, S. Nocentini, D. Martella, C. Parmeggiani, D. S. Wiersma, *Appl. Phys. Lett.* **2019**, *114*, 201103.